Effects of Conjugation in Length and Dimension on Spectroscopic Properties of Fluorene-Based Chromophores from Experiment and Theory

Kiet A. Nguyen,*,†,‡ Joy E. Rogers,*,†,‡ Jonathan E. Slagle,†,§ Paul N. Day,†,‖ Ramamurthi Kannan,†,⊥ Loon-Seng Tan,*,† Paul A. Fleitz,† and Ruth Pachter*,†

Materials and Manufacturing Directorate, Air Force Research Laboratory, Wright Patterson Air Force Base, Ohio 45433

Received: July 6, 2006; In Final Form: September 12, 2006

A series of one-photon absorption spectra for fluorene-based donor–π-acceptor molecules is presented and spectroscopically assigned, based upon the results obtained from time-dependent density functional theory. The computed excitation energies were generally shown to be in good agreement with experiment, particularly when compared to results from measurements carried out in a nonpolar solvent, which were available for some molecules. The computed oscillator strengths may resolve discordant experimental values in some cases, for example, for AF-380, AF-270, and AF-295. However, a quantitative comparison between computed and observed oscillator strengths is complicated by band overlapping. Thus, the computed extinction coefficients obtained by summing over the Gaussian bands are useful in such cases.

Introduction

Donor–acceptor (DA) molecules[1–5] give rise to intramolecular charge-transfer (ICT) excited states that are more stable in polar solvents, as compared to the less polar "locally excited" (LE) states. Nonlinear photophysical responses (e.g., from two-photon absorption) of ICT excited states have a variety of potential applications such as photodynamic therapy,[6] confocal microscopy,[7] fluorescence imaging,[8] optical memory, and microfabrication.[9]

This work focuses on a series of dialkylfluorene-based DA chromophores[10–15] with varied conjugation length and dimension (Figures 1 and 2). Starting with the 9,9-diethylfluorene core and 2-benzothiazolyl as the π-accepting group, the dipolar design extends from diphenylamino (AF-240) to triphenylamino (AF-270) groups (Figure 1). The quadrupolar series of AF-287 and AF-295 extends conjugation length based on the amine core with two identical branches based on AF-240 and AF-270, respectively. Another quadrupolar design (Figure 2) is based on the D–π–A–π–D concept with two diphenylamino groups acting as the electron-donating terminals (AF-389).[16] The first octupolar design of AF-380[17] and AF-350[17,18] is also based on the amine core but with three identical branches based on AF-240 and AF-270, respectively, while the second series is based on the triazine core. In contrast to the first three-arm series of AF-350 and AF-380 with a single electron-rich triarylamine center and π-deficient benzothiazole terminals, the second series of AF-450, AF-455, and AF-457 (Figure 2) have the electron donating end groups and π-centers.[15] The octupolar AF-350 has the same basic structure as AF-380 but is similar to the dipolar AF-270 and the quadrupolar AF-295, having an additional phenyl ring in each branch. Thus, these series based on AF-

240 are designed to probe the effects of conjugation on spectral properties upon going from dipolar (AF-270), to quadrupolar (AF-295) and to octupolar (AF-350) arrangements.[19]

The dialkylfluorene-based DA chromophores have been reported to exhibit strong nonlinear absorption via instantaneous two-photon absorption (TPA)[15–18,20] and excited-state absorption[21,22] after the initial TPA within the duration of a laser (nanosecond) pulse. Thus, there has been considerable interest[11,19,23,24] in establishing structure–property relationships to provide strategies for the design of this class of materials with a suitable OPA and TPA optical response for applications. Except for AF-287, each compound has been studied at least once in the literature. However, a systematic treatment of these families of chromophores, shown in Figures 1 and 2, has not been carried out. Theoretically, these chromophores are presently uncharacterized, except for AF-240.[24–26] In this study, calculations using time-dependent density functional theory (TDDFT)[27] are carried out to interpret and assign the observed spectra and to shed light on the origin of OPA and TPA spectral shifts. A detailed comparison between computed and experimental results from OPA spectra are carried out to assess the accuracy that can be achieved with the computational methods. In addition, computed results for a new three-branched chromophore AF-459-2, which was subsequently synthesized, are presented and compared with the corresponding experimental data.

Computational Methods

Electronic Structure. Although TDDFT has become a useful and widespread tool in predicting excitation energies and oscillator strengths, an underestimation of the excitation energies of ICT states has been reported for functionals with incorrect long-range behavior.[28] Hybrid functionals with a fraction (0.2–28) of the correct Hartree–Fock long-range exchange potential lead to an amelioration. For example, Becke's three-parameter hybrid exhange-correlation functional[29–31] (B3LYP) excitation energies and oscillator strengths do compare favorably with experimental data for some *small* DA systems.[32] Excellent results were obtained for ICT excited state energies of a number

* Corresponding authors. E-mail: Kiet.Nguyen@wpafb.af.mil, Ruth.Pachter@wpafb.af.mil (theoret.), Joy.Rogers@wpafb.af.mil, Loon-Seng.Tan@wpafb.af.mil (expt.).
† Air Force Research Laboratory.
‡ Permanent address: UES, Inc.
§ Permanent address: AT&T Government Solutions.
‖ Permanent address: Anteon Corporation.
⊥ Permanent address: Systran Systems Corporation.

OPA of Fluorene-Based Chromophores

J. Phys. Chem. A, Vol. 110, No. 49, 2006 **13173**
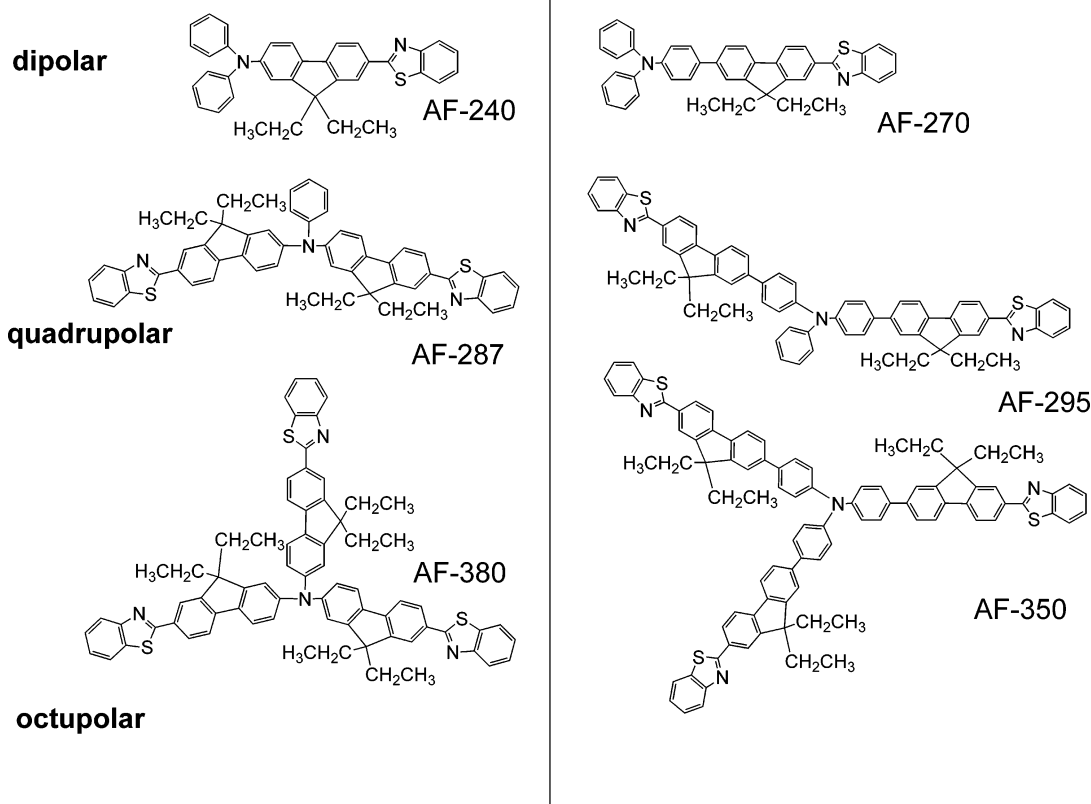
Figure 1. Structures of dipolar, quadrupolar, and octupolar chromophores.

of *small* 7-aminocoumarin derivatives using B3LYP and the hybrid functional of Perdew, Burke, and Ernzerhof (PBE0).[33,34] For dipolar diphenylaminofluorene-based chromophores, the PBE0 excitation energies were found to be in better agreement with experiment, with a mean absolute error (MAE) of 0.14 eV using the 6-31G(d) basis set.[25] The importance of the long-range corrected (LC) functionals to account for charge-transfer excitations has been recognized and is being addressed, for example, by Tawada et al.,[35] Yanai et al.,[36] and others.[37,38]

The computed excitation energies tabulated in Tables 1 and 2 were carried out with the PBE0 functional using TDDFT[39−42] as implemented in the Gaussian 03[43] programs. The TDDFT calculations were carried out at the B3LYP/6-31G* optimized structures, using the same basis set as used in the ground-state DFT calculations, since the basis effects were found to be rather small (see Table 1). Note also that eliminating the set of d polarization functions from each of the carbon atoms does not significantly affect the excitation energy and oscillator strength. To gauge the effects of solvent, we applied the polarizable continuum model[44,45] (PCM) in conjunction with TDDFT (using a static dielectric of 7.58 and an optical-frequency dielectric constant of 1.971) to compute excitation energies and oscillator strengths for AF-240 in THF solution. The solute is placed in a cavity formed by a union of spheres centered on each atom according to the united atom topological model (UA0) and empirical solvent radii of 2.56 Å for THF. The ground- and excited-state dipoles are computed using the finite field method with an applied field of ±0.0001 au. The 3D molecular orbitals were generated by using the GAMESS program[46] and its graphic package.[47]

One-Photon Intensity. The computed oscillator strength is related to the experimental integrated intensity by

$$f_{0f} = 4.32 \times 10^{-9} \int \epsilon(\tilde{\nu}) \, d\tilde{\nu} \quad (1)$$

where the extinction coefficient ϵ and frequency $\tilde{\nu}$ are in units of L·mol^{-1}·cm^{-1} and cm^{-1}, respectively. Since the integration limits in eq 1 are generally not known, a single Gaussian function was used to represent an experimental spectral band that gives rise to an approximate measure of the corresponding band intensity:

$$f_{0f} = 4.32 \times 10^{-9} \epsilon_{max} \int \exp\left[\frac{-4\ln 2}{\tilde{\nu}_{fwhm}^2}(\tilde{\nu} - \tilde{\nu}_f)^2\right] d\tilde{\nu} =$$

$$\frac{4.32 \times 10^{-9}\sqrt{\pi}}{2\sqrt{\ln 2}}\epsilon_{max}\tilde{\nu}_{fwhm} \quad (2)$$

where $\tilde{\nu}_{fwhm}$ is the full-width at (fwhm) half-maximum ($\epsilon_{max}/2$) in cm^{-1}. Thus, the spectral cross section (in cm^2, $\sigma(\tilde{\nu}) = 3.83 \times 10^{-21} \epsilon(\tilde{\nu})$) or extinction coefficient can be readily obtained from the computed oscillator strengths:

$$\epsilon(\tilde{\nu}) = \frac{2\sqrt{\ln 2}}{4.32 \times 10^{-9}\sqrt{\pi}} \sum_f \frac{f_{0f}}{\tilde{\nu}_f^{fwhm}} \exp\left[\frac{-4\ln 2}{(\tilde{\nu}_f^{fwhm})^2}(\tilde{\nu} - \tilde{\nu}_f)^2\right]$$

$$(3)$$

provided their bandwidths are known. The computed extinction coefficients (eq 3) and experimental oscillator strengths (eq 2) listed in Table 2 are obtained using the *full* bandwidth at half-maximum for $\tilde{\nu}_{fwhm}$. The oscillator strength obtained using $\tilde{\nu}_{fwhm}$ as twice the half width measured on the low-energy side is comparable to the corresponding value using the *full* bandwidth for a somewhat symmetric OPA band of AF-240. This is not true for other chromophores due to the band overlapping. In the case of integration over only the S$_1$ absorption band that is well isolated from higher-energy bands, the upper limit in eq 1 can be approximated by the frequency of the minimum intensity between S$_1$ and S$_n$ bands. Using Gauss−Chebyshev integra-
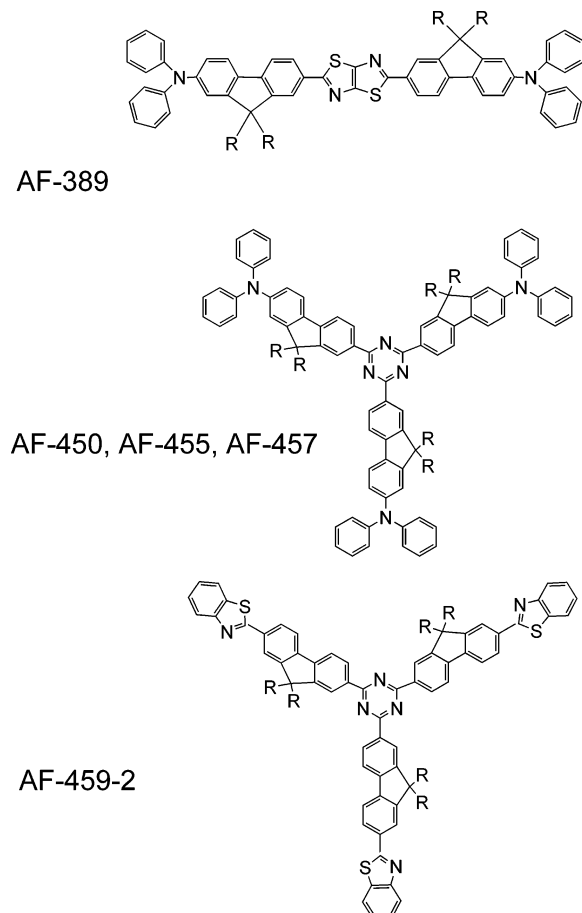
Figure 2. AF-389 (R = decyl), AF-450 (R = decyl), AF-457 (R = prop-2-enyl), (AF-455, R = 3,7-dimethyoctyl), and AF-459-2 (R = ethyl).

TABLE 1: Computed OPA Results for the PBE0 ($x-c$) Functional with Different Basis Sets

molecule	PBE0/6-311+G(d,p)		PBE0/6-31G(d)	
	energy	f	energy	f
AF-240				
2^1A	2.99	1.00	3.05	0.99
3^1A	3.65	0.01	3.90	0.01
4^1A	3.89	0.49	3.96	0.55
5^1A	3.94	0.18	4.14	0.20
6^1A	4.04	0.02	4.19	0.04

molecule	PBE0/6-31G(d)		PBE0/6-31G	
	energy	f	energy	f
AF-457				
1^1E	2.90	1.22	2.84	1.15
2^1A	3.04	0.00	2.96	0.00
3^1A	3.07	0.00	2.99	0.00

tion[48] with this frequency limit for AF-459-2 leads to f_{01} of 3.22. This is well approximated by a Gaussian line shape with f_{01} = 3.33. Thus, all experimental oscillator strengths are computed using eq 2, unless mentioned otherwise. The computed oscillator strengths for doubly degenerate excited states are multiplied by a degeneracy factor of 2 for direct comparison with experiment.

Experimental Methods

Synthesis of AF-240, AF-287, AF-380; AF-270, AF-295, AF-389; AF-450, AF-455, AF-457; and AF-459-2. AF-240[14] as well as AF-450, AF-455, and AF-457[15] were prepared

according to the procedures that were previously described. AF-287 was synthesized by the palladium-catalyzed double amination of aniline with 2-(7-bromo-9,9-diethylfluoren-2-yl)-benzothiazole (abbreviated as BT-Fl(Et$_2$)-Br). The latter is also a key intermediate used in the preparations of AF-240, AF-270, AF-295, and AF-350. Thus, the reaction of BT-Fl(Et$_2$)-Br in the presence of a palladium catalyst with a Stille reagent generated from 4-bromotriphenylamine, *n*-butyllithium, and tri-*n*-butylstannyl chloride led eventually to AF-270. Similarly, AF-295 was prepared from the Pd-catalyzed, double amination of 4,4′-dibromotriphenylamine and a Suzuki reagent generated from BT-Fl(Et$_2$)-Br, *n*-butyllithium and triisopropylborate. AF-350 was obtained from the same Suzuki reagent and 4-(7-benzothiazol-2-yl-9,9-diethylfluoren-2-yl)phenyl]bis(4-bromophenyl)amine, which was prepared via a regiospecific bromination of two unsubstituted para positions of the triphenylamino end of AF-270 with *N*-bromosuccinamide in *N*,*N*-dimethylforamide (DMF). Finally, AF-380 was prepared from a copper-catalyzed, Ullmann amination reaction of 2-(7-amino-9,9-diethylfluoren-2-yl)benzothiazole with 2 equiv of 2-(7-iodo-9,9-diethylfluoren-2-yl)benzothiazole. The latter was prepared in two steps from 7-bromo-9,9-diethylfluorene-2-carboxaldehyde[14] via (a) nickel-catalyzed iodo-bromo exchange reaction and (b) condensation of the resulting iodo-aldehyde precursor with 2-aminothiophenol in dimethyl sulfoxide (DMSO).

The new triazine-containing AF-459-2 was made by cyclotrimerization of the 7-(2-benzothiazolyl)-9,9-diethylfluorene-2-carbonitrile precursor in trifluoromethanesulfonic acid. The nitrile was obtained from the corresponding bromofluorene (BT-Fl(Et$_2$)-Br) by the reaction with copper(I) cyanide.

7-(2-Benzothiazolyl)-9,9-diethylfluorene-2-carbonitrile. A mixture of 2-(7-bromo-9,9-diethylfluoren-2-yl)benzothiazole (8.68 g, 0.02 mol), copper(I) cyanide (Aldrich, 2.25 g, 0.025 mol), and *N*-methyl-2-pyrrolidinone (38 mL) was kept under reflux for 2 h, cooled, and poured into a mixture of ice (110 g) and 28% ammonium hydroxide (110 mL). The mixture was stirred for 1 h and filtered. The solids were washed with dilute ammonium hydroxide and then with water to get the crude product, 7.64 g. This crude product was purified by chromatography over silica gel, elution of the column with toluene, and recrystallization from a mixture of toluene and heptane, 6.60 g (87% yield), mp 199−200 °C. MS *m/z* (relative intensity): 380 (M$^+$). Anal. Calcd for C$_{25}$H$_{20}$N$_2$S: C, 78.91; H, 5.30; N, 7.36; S, 8.43%. Found: C, 78.95; H, 5.51; N, 7.42; S, 8.35%. ^{1}H NMR (CDCl$_3$, δ): 0.31−0.36 (t, 6H), 2.06−2.22 (m, 4H), 7.26−7.54 (m, 2H), 7.64−7.67 (m, 2H), 7.90−7.93-(1H), 8.05−8.18 (m, 3H). ^{13}C NMR (CDCl$_3$, δ); 8.45, 32.48, 56.93 (sp^{3}C), 110.8, 119.5, 120.8, 121.3, 121.6, 121.7, 123.2, 125.4, 126.6, 127.5, 131.5, 134.1, 135.0, 142.3, 145.0, 151.3, 151.5, 154.2, 167.8 (sp^2 and sp C).

2,4,6-Tri-[7-(benzothiazol-2-yl)-9,9-diethylfluoren-2-yl]triazine, AF-459-2. Trifluoromethanesulfonic acid (Lancaster, 5 mL) was cooled with stirring in an ice-salt bath. 7-(2-Benzothiazolyl)-9, 9-diethylfluorene-2-carbonitrile (1 g) was added in several portions, and the mixture was stirred for 24 h, allowing it to warm to room temperature. The mixture was then poured into a mixture of ice and water to get a yellow slurry that became colorless on addition of ammonium hydroxide. This was filtered and washed with water to get the crude product, 1.06 g, mp 171−178 °C. Column chromatography of the crude product over silica gel and elution with toluene gave first some

TABLE 2: TD-PBE0/6-31G(d) Excitation Energies (in eV, values in parentheses are energies at ϵ_{max}), Oscillator Strengths (f), and ϵ_{max} (in L·mol⁻¹·cm⁻¹) Compared with Other Calculations and with Experimental Results

molecule	energy (theory)	$f(\epsilon_{max})$ (theory)	energy (exp)	$f(\epsilon_{max})$ (exp)	solvent	ref	molecule	energy (theory)	$f(\epsilon_{max})$ (theory)	energy (exp)	$f(\epsilon_{max})$ (exp)	solvent	ref
AF-240[a]							**AF-240[a]**						
2^1A	3.05 (3.06)	0.99 (5.87×10^4)	3.17	0.76 (4.44×10^4)	THF	this work	4^1A	3.96 (4.02)	0.55 (2.56×10^4)	4.07	0.75 (2.48×10^4)	THF	this work
			3.08		hexane	50				4.04		hexane	50
			3.15	0.57 (4.54×10^4)[b]	THF	52				3.91		THF	52
			3.15	0.77 (4.82×10^4)	toluene	52				3.99[b]	(2.49×10^4)[b]	THF	14
			3.17[b]	0.75 (4.34×10^4)[b]	THF	14	5^1A	4.14	0.20				
3^1A	3.90	0.01					6^1A	4.19	0.06				
AF-287							**AF-287**						
2^1A	2.86 (2.92)	1.39 (7.35×10^4)	2.97	1.57 (7.09×10^4)	THF	this work	5^1A	3.80	0.01				
			2.95		hexane	50	6^1A	3.88 (3.87)	0.87 (4.56×10^4)	3.97	3.64×10^4	THF	this work
3^1A	3.14	0.36	~3.2[c]		THF	this work				3.97		hexane	50
			3.08[c]		hexane	50	7^1A	4.10	0.04				
4^1A	3.78	0.41	~3.8[c]		THF	this work							
AF-380							**AF-380**						
1^1E	2.83 (2.83)	2.43 (1.61×10^5)	2.90	1.90 (1.24×10^5)	THF	this work	3^1A	3.73	0.00				
			2.91[b]	3.70 (2.43×10^5)[b]	THF	17	4^1A	3.76	0.91				
			2.89		hexane	50	5^1A	3.76 (3.76)	0.91 (6.39×10^4)	3.87	1.71 (6.02×10^4)	THF	this work
			2.90[b]	0.18 (1.16×10^4)[b]	THF	9				3.84[b]	3.33 (1.17×10^5)[b]	THF	17
			2.87[b]	~0.15 (1.14×10^4)[b]	THF	51				3.87[b]	0.17 (5.60×10^3)[b]	THF	9
2^1A	3.22	0.02	3.05		hexane	50							
AF-389[e]							**AF-389[e]**						
1^1A_u	2.59 (2.60)	2.36 (1.34×10^5)	2.84	1.73 (9.78×10^4)	THF	this work	4^1A_g	3.88					
			2.84[b]	1.75(9.82×10^4)[b]	THF	16	5^1A_g	4.10					
2^1A_g	2.91		2.90[b]		THF	16	6^1A_u	4.11 (3.75)	0.38 (2.63×10^4)	4.03	(3.91×10^4)	THF	this work
2^1A_u	3.41	0.43								4.03[b]	(4.45×10^4)[b]	THF	16
3^1A_g	3.45						6^1A_g	4.11					
3^1A_u	3.65	0.25					7^1A_u	4.18	0.07				
4^1A_u	3.88	0.02					7^1A_g	4.19					
AF-270							**AF-270**						
2^1A	3.05 (3.11)	1.02 (5.45×10^4)	3.29	1.31 (6.07×10^4)	THF	this work	4^1A	3.94	0.17				
			3.30[b]	2.33 (1.53×10^5)[b]	THF	17	5^1A	3.99	0.01				
3^1A	3.67 (3.72)	0.94 (4.07×10^4)	4.08	(3.12×10^4)	THF	this work	6^1A	4.17	0.22				
AF-295							**AF-295**						
2^1A	2.94 (3.00)	1.63 (1.19×10^5)	3.21	2.79 (1.02×10^5)	THF	this work	6^1A	3.86	0.06				
			3.25	5.23 (1.90×10^5)	THF	17	7^1A	3.92	0.02				
3^1A	3.11	0.34					8^1A	3.95	0.04				
4^1A	3.61	0.52					9^1A	3.98	0.19				
5^1A	3.63 (3.62)	1.47 (8.65×10^4)	~3.5	(6.8×10^4)	THF	this work							
AF-350							**AF-350**						
1^1E	2.93 (2.96)	2.93 (1.90×10^5)	3.15	2.39[d] (1.52×10^5)	THF	this work	3^1A	3.58	1.56				
			3.18	4.18[d] (2.63×10^5)	THF	17	4^1A	3.58 (3.58)	1.56 (1.06×10^5)	3.56	(9.00×10^4)	THF	this work
			3.15	2.27[d] (1.56×10^5)	THF	52				3.55		THF	17
			3.15	2.13[d] (1.45×10^5)	toluene	52				3.54		THF	52
			3.14	3.97[d] (2.66×10^5)	THF	18				3.54		toluene	52
2^1A	3.15	0.00											
AF-457[f]							**AF-457[f]**						
1^1E	2.90 (2.91)	2.44 (1.46×10^5)	2.99	1.96 (1.18×10^5)	THF	this work	2^1A	3.04	0.00				
			2.99	2.87 (1.68×10^5)[b]	THF	15	2^1E	3.07	0.01				
AF-450[g]							**AF-450[g]**						
1^1E	2.91 (2.92)	2.49 (1.49×10^5)	2.98	1.88(1.15×10^5)	THF	this work	2^1A	3.05	0.00				
			2.98	2.21(1.32×10^5)[b]	THF	15	2^1E	3.08	0.00				
AF-459-2							**AF-459-2**						
$1^1E'$	3.23 (3.23)	4.60 (3.35×10^5)	3.20	3.33 (2.46×10^5)	THF	this work	$3^1A'$	3.83					
$2^1A'$	3.38						$3^1E'$	3.84 (3.84)	0.56 (4.23×10^4)	3.88	(4.14×10^4)	THF	this work
$2^1E'$	3.45	0.00					$4^1E'$	4.01	0.04				

[a] Energy and oscillator strength (f) for AF-240: 2.90 (1.10), 3.87 (0.610), 3.96(0.02), 4.11(0.26), 4.12(0.08) from TD-PCM-PBE0/6-31G(d)//PCM-B3LYP/6-31G(d) with THF as the solvent; 3.57 (1.42), 4.35 (0.02), 4.43 (0.09), 4.56 (0.25) 4.66 (0.01) from TD-CAMB3LYP/6-31G(d)//B3LYP/6-31G(d); 3.58, 4.36, 4.42, 4.55 from TD-CAMB3LYP/6-31G(d)//B3LYP/6-31G(d);[26] 2.86 (0.907) from TD-B3LYP/6-31G(d,p)//B3LYP/6-31G(d,p).[24] [b] Data have been obtained by digitization from spectrum in cited reference. [c] Shoulder. [d] Oscillator strength evaluated using twice the half-width measured on the low-energy side. [e] Computed with R = ethyl. [f] Computed 6-31G energy and oscillator strength (f): 2.84 (2.30), 2.96 (0.00), 2.99 (0.01), 3.02 (0.00), 3.77 (0.91), 3.77 (0.00), 3.94 (0.00). [g] Computed with R = propyl. Computed 6-31G energy and oscillator strength (f): 2.85 (2.36), 3.04 (0.00), 3.07 (0.01).

starting nitrile (0.12 g) and then the triazine product (0.5 g). This was recrystallized from a mixture of toluene and heptane, 0.48 g (48% yield), mp 224−227 °C. MS *m/z* (relative intensity) 1140 (M^+). Anal. Calcd for $C_{75}H_{60}N_6S_3$: C, 78.91; H, 5.30; N, 7.36; S, 8.43%. Found: C, 78.52; H, 5.50; N, 7.66; S, 8.35%. ¹H NMR (CF_3COOD, δ): 0.10 (t, 18H), 2.17 (m 12H), 7.59−7.69 (m, 6H), 7.85−7.99 (m, 6H), 8.02−8.13 (m, 12H), 8.57−8.66 (m, 6H). ¹³C NMR (δ): 9.58, 34.88, 60.57 (sp^3C), 119.91, 125.12, 125.35, 125.69, 125.98, 127.94, 128.14, 131.09, 132.00, 132.08, 133.00, 133.38, 133.53, 142.99, 150.33, 150.82, 155.95, 157.20, 171.42, 177.07 (sp^2C).

Spectroscopy. Ground-state UV/Vis absorption spectra were measured on a Cary 500 spectrophotometer. All data was measured in THF at room temperature in 1 cm cuvettes, by preparing three independent stock solutions of each and varying the concentration accordingly.
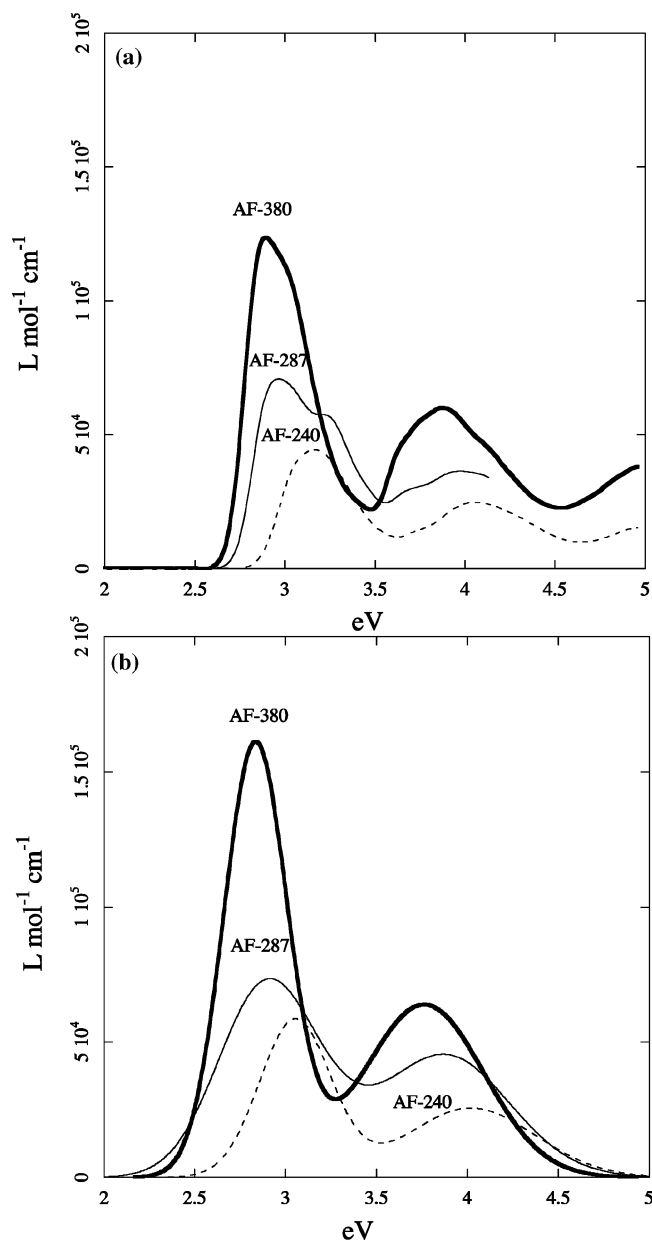
Figure 3. Experimental (in THF; a) and computed (b) OPA spectra of AF-240 (dashed, fwhm = 0.46 eV for S_1, fwhm = 0.81 eV for S_2–S_n), AF-287 (solid, fwhm = 0.60 for S_1–S_2, fwhm = 0.81 eV for S_3–S_n), AF-380 (bold, fwhm = 0.41 eV for S_1–S_2, fwhm = 0.77 eV for S_3–S_n).

Results

AF-240, AF-287, and AF-380. The OPA and TPA spectral interpretation of AF-240 and other dipolar AF-X molecules has been given in previous studies.[25,26] Therefore, we briefly review the AF-240 spectrum (Figure 3) and then discuss the conjugation and multibranching effects upon the spectra. Experimentally, the OPA spectrum of AF-240 taken in THF has two broad bands. In hexane, the low-energy band splits into two peaks located at 3.08 eV (Table 2) and 3.22 eV. The latter was assigned to a vibronic progression. These bands are overlapped in THF, which causes a blue-shift in the maximum (to 3.17 eV, $f = 0.76$) instead of the normal red-shift typically observed for an ICT band in a polar solvent. The ICT band arises largely from the HOMO to LUMO one-electron transition (see Figure 4), with the predicted energy of 3.05 eV and oscillator strength of about 1. It is worthwhile to note that the corresponding CAMB3LYP excitation energy is 3.57 eV ($f = 1.42$), in

agreement with the computed (at the B3LYP/6-31G geometry) value of 3.58 eV reported by Rudberg et al.[26] The CAMB3LYP results and discussion for molecules in Tables 1 and 2, obtained with the Dalton program,[49] are included in Table 1S of the Supporting Information. For AF-240, CAMB3LYP overestimates the excitation energy and oscillator strength for the first ICT transition of AF-240 by a significant amount, even after accounting for the effects of solvents (see below) and the effects of diffuse functions with the triple-ζ basis set (Table 1). While the predicted PBE0 excitation energy is in excellent agreement with the experimental value of 3.08 eV in hexane, the corresponding oscillator strength and ϵ_{max} appear to be overestimated as compared to values obtained in toluene and THF. The TDDFT excitation energy with the PCM model is slightly (0.15 eV) red-shifted in THF while the corresponding oscillator strength is slightly (0.1) increased. The next band is broad and featureless in both THF and hexane. There are several electronic transitions that may contribute to this broad band located at about 4 eV (see Table 2). The computed transition at 3.96 eV with an oscillator strength of 0.55 is predicted to have a dominant contribution to the intensity of this high-energy band. The total computed oscillator strength of 0.8 for the four transitions in the region is in good agreement with the experimental values of 0.6–0.8 obtained in THF.

Spectra of AF-287, a two-branched version of AF-240, taken in hexane and THF reveal the first bands at 2.95 and 2.97 eV, respectively. Thus, the double branching of AF240 produces a red-shift of 0.13 eV for the first excited state. This is slightly smaller than the computed red-shift of 0.19 eV (Table 2). Note that the LUMO-LUMO+1 gap (see Figure 4) in the two-branched system is much smaller than the corresponding gap in the AF-240 DA complex. Thus, the S_2 (3.14 eV) excitation energy of AF-287 is predicted to arise from the HOMO → LUMO+1 one-electron transition at slightly higher than that of S_1 (2.86 eV). This is consistent with the experimental band at 3.08 eV observed in hexane and a shoulder at ~3.2 in THF. The predicted total oscillator strengths of the two transitions of 1.8 is in good agreement with the experimental value of 1.6 obtained by integrating the full band envelope over the low- and high-energy sides. Note that the oscillator strength estimated by using only the lower (energy) half of the band envelope is reduced by a factor of 2 due to band overlapping. Although the observed band overlapping prevents us from extracting accurate oscillator strengths for the individual bands without extensive deconvolution, it appears to confirm the presence of two transitions predicted by TDDFT. In hexane, the next well-resolved peak appears at 3.28 eV. This band, not observed in THF, appears to be vibronic in nature. The higher energy region of the spectrum has a broad band with its maximum at 3.97 eV and a shoulder at about 3.8 eV. TDDFT predicts a number of states in this region. Two strong transitions predicted to occur at 3.78 and 3.88 eV can account for the observed features.

The spectrum of AF-380 in THF (Figure 3) has two broad peaks located at 2.90 and 3.87 eV. The first band has a shoulder on the high-energy side, which is better resolved in hexane.[50] TDDFT predicts a doubly degenerate and intense transition at 2.83 eV (1^1E) for the first excited state, which arises from the HOMO → LUMO+1 one-electron transition. The predicted excitation energy is in good agreement with the experimental values (2.87–2.91 eV) reported for the first band. The predicted oscillator strength of 2.4 is in reasonable agreement with our experimental value of 1.9, as approximated using the full band envelope in THF. However, we found very large discrepancies among the experimental values obtained from digitization of

OPA of Fluorene-Based Chromophores

J. Phys. Chem. A, Vol. 110, No. 49, 2006 **13177**
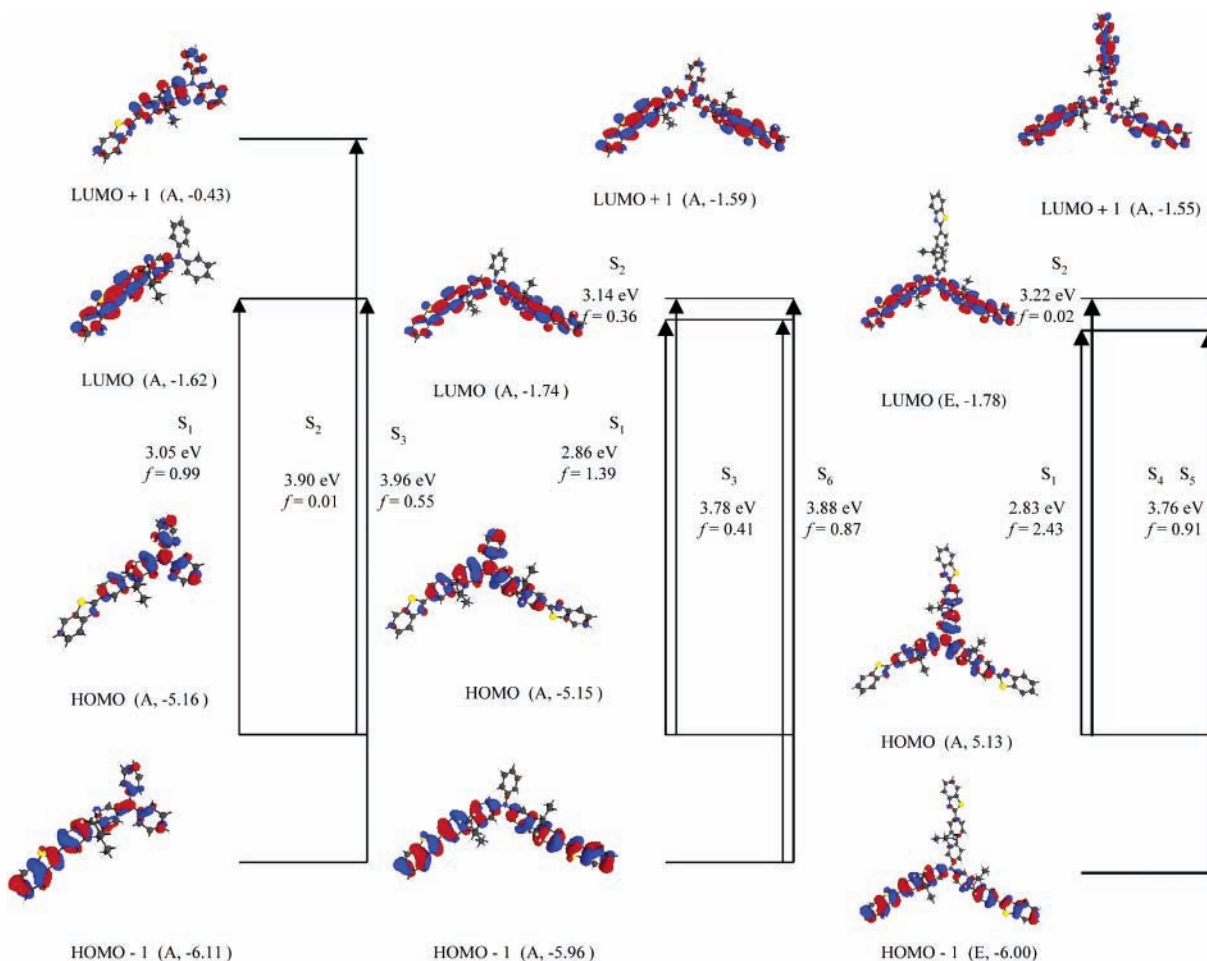
Figure 4. Molecular orbital diagrams for AF-240, AF-287, and,AF-380. Solid arrows denote the major one-electron excitations.

the previously reported spectra in the *same* solvent (see Table 2). Our estimate of the extinction coefficients are larger than values reported by Kirkpatrick et al.[9] and Joshi et al.[51] but much smaller than the values reported by He et al.[17] In view of the structure of AF-380 with a three-arm relationship to AF-240, our estimate of the extinction coefficients of about 2−3 times that of AF-240 seems reasonable. The extinction coefficients smaller than the corresponding values of AF-240 appear to be disconcerted.

The second excited state is predicted to occur at 3.22 eV (2^1A). Although this band may be correlated with the peak observed at 3.05 eV in hexane,[50] the small calculated oscillator strength (0.02) suggests that the second observed peak is largely vibronic in nature. The third and fourth excited states are predicted to occur at 3.72 and 3.76 eV. The latter is accidentally degenerate with the fifth excited state. Based on their combined oscillator strength (1.8), these two transitions are likely to have dominant contributions in the observed strength (1.42) in the present work in THF.

Because of the C3 octupolar arrangement, total dipole moments of the ground (0.55 D) and first excited (1.90 D) state are much smaller than in other DA chromophores. Thus, contributions from the transition between the first excited state to nearby excited states are likely to be crucial for a quantitative treatment of the TPA cross section, which will be reported later.

AF-389. The AF chromophores discussed above have electron-accepting (benzothiazolyl) and electron-donating groups (diphenylamine) connected to a dialkylfluorene core. AF-389 with a thiazolothiazole bifluorene center and two diphenylamine terminals represents a D−π−A−π−D structural arrangement. The two dialkylfluorene units can be in a *Z* or *E* conformations. However, their excitation energies and oscillator strengths are found to be similar and the spectral properties of the *E* conformer with C_i symmetry are given in Table 2. The OPA spectrum of AF-389 taken in THF has two absorption peaks at 2.84 and 4.03 eV (Figure 5). The former has about twice the intensity of the latter. The low-energy band has a shoulder at about 2.7 eV, which is assigned to the first electronic transition. The computed (for the diethyl analog) excitation energy of 2.6 eV is in good agreement with the observed values.[16] The predicted oscillator strength of 2.4, however, is significantly larger than the experimental values of 1.7−1.8 in THF for the decyl analogue. The second excited state is predicted to be OPA "forbidden" with the same (A_g) symmetry as the ground state. This TPA "allowed" 2^1A_g state is predicted to occur at 2.91 eV and, therefore, absorbs two photons at 1.45 eV. This is consistent with the TPA maxima observed at 1.45 and 1.57 eV in THF.[16] The latter TPA maximum is significantly (0.3 eV) blue-shifted from the observed OPA maxium at 2.84 eV and, therefore, has been speculated[16] to have a different origin. Our preliminary TPA results show a large absorption cross-section for the 2^1A_g state.

AF-270, AF-295, and AF-350. This series of chromophores have the same electronic rich center as in the AF-240, AF-287, and AF-380 discussed in the previous section but with an additional phenyl ring in each branch. For the dipolar arrangement of AF-270, adding a phenyl ring to AF-240 does not appear to induce significant changes in color and intensity, as predicted by TDDFT. Experimentally, a small increase in energy (0.12
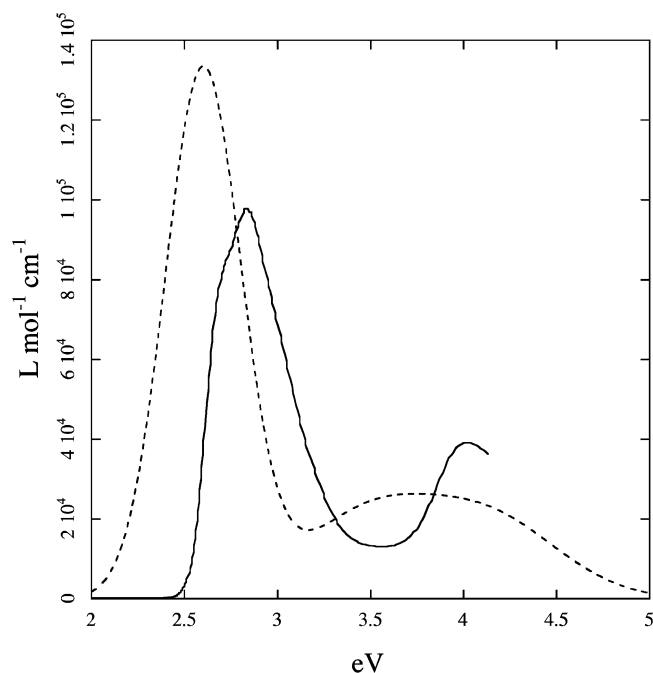
Figure 5. Experimental (solid, in THF) and computed (dashed, fwhm = 0.48 eV for S_1–S_2, fwhm = 0.81 eV for S_3–S_n) OPA spectra of AF-389.

eV) and a large increase in oscillator strength (0.55) are observed in THF upon going from AF-240 to AF-270. The large increase in oscillator strength can be attributed to the asymmetry of the band envelope due to the overlapping with higher energy bands, as revealed by a large difference between the fwhm (0.58 eV) and twice the half-width (thw) measured on the low-energy side (0.43 eV). In contrast, the absorption band of AF-240 is more symmetric, with comparable fwhm (0.46 eV) and thw (0.41 eV) values. Note that the energy of our experimental spectral maximum is essentially identical to the value reported by He et al.[17] in the same solvent. The measured extinction coefficient is in good agreement with the computed results (see Table 2 and Figure 6) but is less than half the value from previous experiment.[17] As expected, AF-270 exhibits similar ICT char-acteristics to those found in AF-240. This is reflected in the similarity of the electron distribution in the two dyes (cf. Figures 4 and 7).

Similar to AF-287, AF-295 (Figure 1) is designed to extend conjugation length based on the triphenylamine core with two identical branches based on AF-270. However, the HOMO and LUMO, largely localized on triphenylamine and benzothiazolyl rings, are not significantly delocalized; their energies are not significantly shifted with the added phenyl rings (Figure 7). The ICT is found to originate from the triphenylamine core to the benzothiazolyl π-accepting groups (Figure 7), analogous to AF-287 (Figure 4). The first excited state is predicted to be slightly (0.1 eV) red-shifted upon going from one to two branches, in good agreement with experiment. TDDFT predicted an excita-tion energy of 2.94 eV for the first excited state, 0.27 eV lower than the first spectral maximum (3.21 eV) observed in THF. The large deviation may be attributed to spectral broadening due to the convolution of nearby electronic transitions (see Table 2). Thus, the computed spectral maximum (3.00 eV) and ϵ_{max} (1.19 × 10^5) are in a better agreement with the corresponding experimental values. However, our measured ϵ_{max} of 1.02 × 10^5 in THF is about half the value obtained from the spectrum reported recently.[17] In the higher energy region, electronic
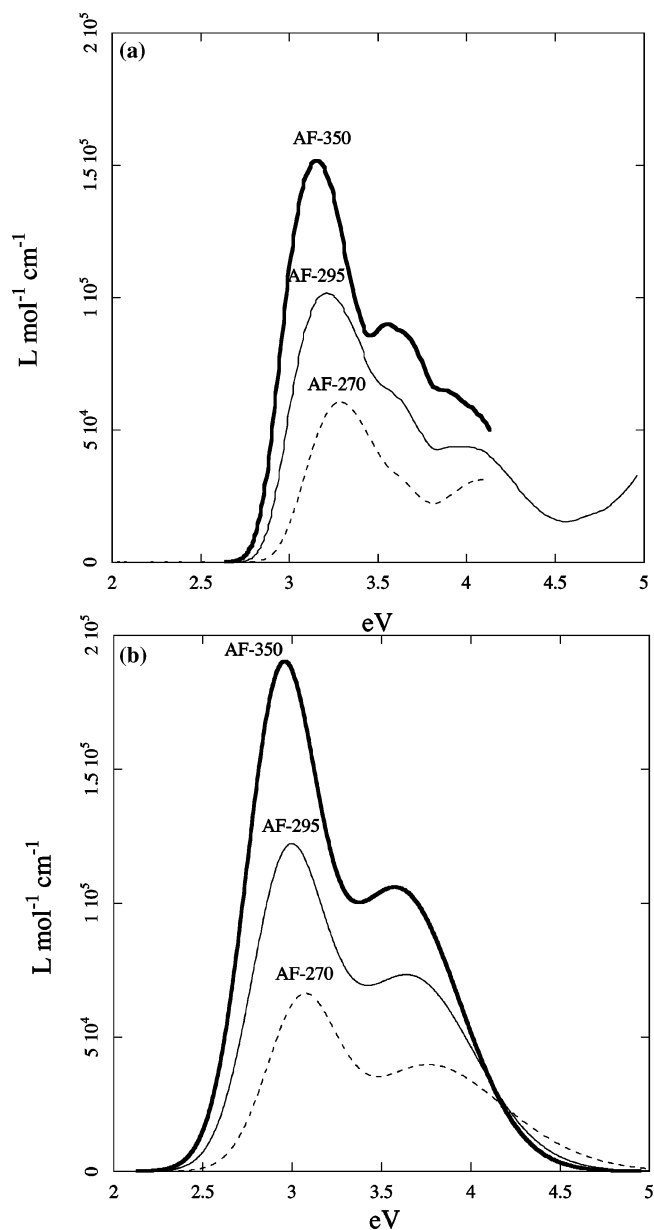
Figure 6. Experimental (in THF; a) and computed (b) OPA spectra of AF-270 (dashed, fwhm = 0.46 eV for S_1–S_3, fwhm = 0.81 eV for S_4–S_n), AF-295 (solid, fwhm = 0.46 eV for S_1–S_3, fwhm = 0.81 eV for S_4–S_n), AF-350 (bold, fwhm = 0.46 eV for S_1–S_2, fwhm = 0.81 eV for S_3–S_n) in THF.

transitions are predicted to be more closely spaced. This is consistent with a shoulder occurring at about 3.5 eV in the spectrum.

The octupolar design of AF-350 is also based on the triphenylamine core but with three identical branches based on AF-270, in analogy to AF-380. However, the two octupolar dyes do not appear to share common spectral features, except for the first band with the maximum at 3.15 eV observed in THF (cf. Figures 3 and 6). The first transition is predicted to be an ICT state with an excitation energy of 2.94 eV, in reasonable agreement with experiment. The corresponding oscillator strength of 3.2 is significantly larger than the value of 2.4 obtained from thw as measured on the low-energy side in THF due to the overlapping of first and second band envelopes (see Figure 6). The band overlapping results in a slight blue-shift from excitation energy in the spectral maximum for the first band using the sum of Gaussian expression (see Table 2), which gives a reasonable estimate (1.90 × 10^5) for the first ϵ_{max} as compared

OPA of Fluorene-Based Chromophores

J. Phys. Chem. A, Vol. 110, No. 49, 2006 **13179**
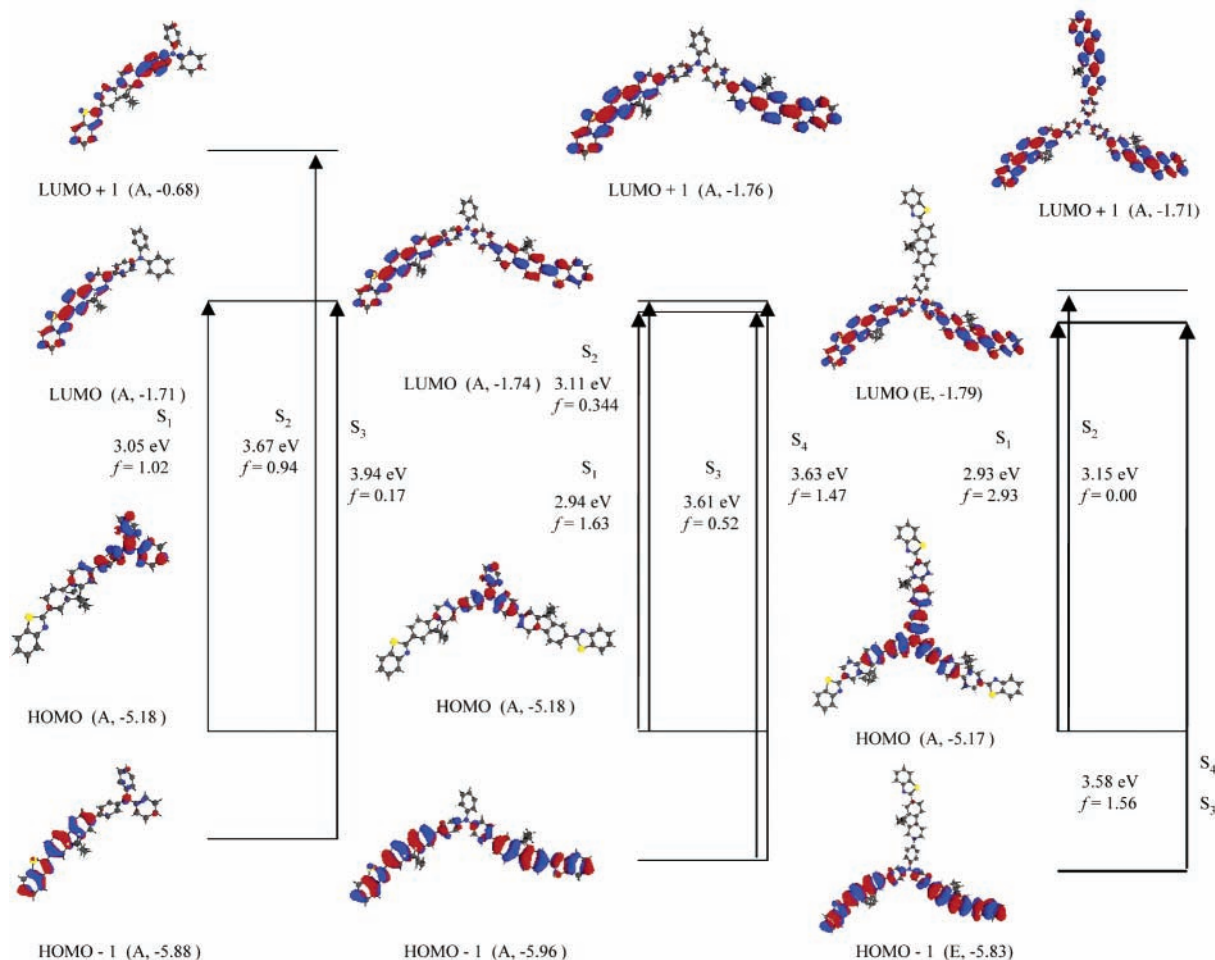
Figure 7. Molecular orbital diagrams for AF-270, AF-295, and,AF-350. Solid arrows denote the major one-electron excitations.

to the experiment. Note that the present experimental extinction coefficient and the oscillator strength in THF are in good agreement with values from Rumi and Perry[52] but significantly smaller than values obtained by digitization of the spectra reported by He et al.[17,18] Again, our estimate of the extinction coefficients of about 3 times that of AF-270 seems reasonable in view of the structural relationship of AF-350 to AF-270. In the higher energy region of the spectrum, there are noticeable differences between the two short- and long-arm chromophores. While the second band of AF-380 in THF is broad with a maximum at 3.87 eV, for AF-350, it is red-shifted to 3.56 eV. The 0.3 eV shift observed in THF is consistent with the predicted shift of 0.2 eV.

AF-450, AF-455, and AF-457. The AF-45X chromophores have three diphenylaminofluorenyl groups connected to the central 1,3,5-triazabenzene core with different alkyl groups attached to the fluorene units (Figure 2). In THF, the OPA absorption spectra (Figure 8) of these chromophores are similar with broad maxima at about 3.0 eV for the first band.[15] A maximum at 2.97 eV from a spectrum taken in hexane for AF455 (R = 3,7-dimethyloctyl) is slightly red-shifted.[22] The spectrum also revealed an additional peak slightly higher in energy. In the calculations, we consider two triazine-based chromophores with different side chains. AF-457 has two prop-2-enyl side chains while AF-450 and AF-455 have the long linear and branched decyl side chains, respectively. These long alkyl side chains are modeled by propyl groups. The first excited states of AF-457 and AF-450 (propyl analog) are predicted to occur at about 2.9 eV, in good agreement with experiment. The total predicted oscillator strengths of about 2.4 for the doubly

degenerate transitions of these systems are slightly larger than our corresponding experimental values (1.9−2.0), which are smaller than values obtained from the digitization of the spectra[15] in the same solvent. Note that these doubly degenerate first excited states are predicted to be nearly degenerate with three other transitions. These weakly allowed bands at slightly higher energy might explain an additional peak observed in hexane.[22] A solvatochroism study of AF455[22] also indicated an ICT character of the first excited state. TDDFT results appear to confirm the experimental findings. The MO diagrams (Figure 9) illustrate the ICT characteristic for the first and second excited states. Note that the first ICT transitions are made up of the HOMO and the nearby degenerate HOMO-1, in contrast to simple HOMO−LUMO one-electron transitions found in other AF-X molecules. Because of the near planar structure with C3 symmetry, these systems do not have significant net dipoles in the ground (0.04 D for AF-457) and first excited (1.03 for AF457) states. The angle (69°) between transition dipole and the dipole difference is also not optimal for TPA. However, the couplings of the first excited state with nearby transitions is likely responsible for the observed TPA.[15]

AF-459-2. Finally we consider AF-459-2, a planar molecule with a verified C_{3h} symmetry, which is predicted to have the S_0-S_1 transition at 3.23 eV from the ground A′ to the first ^{1}E′ excited state. This is a strongly allowed transition with the combined f larger than 4. The next higher transition (S_0-S_2) is predicted to occur at about 3.4 eV with A′ symmetry, which is symmetry-forbidden in the OPA selection rule but might have significant TPA intensity. Another notable feature in the AF-459-2 is the reduction in intensity of the higher energy transitions

13180 *J. Phys. Chem. A, Vol. 110, No. 49, 2006*

Nguyen et al.
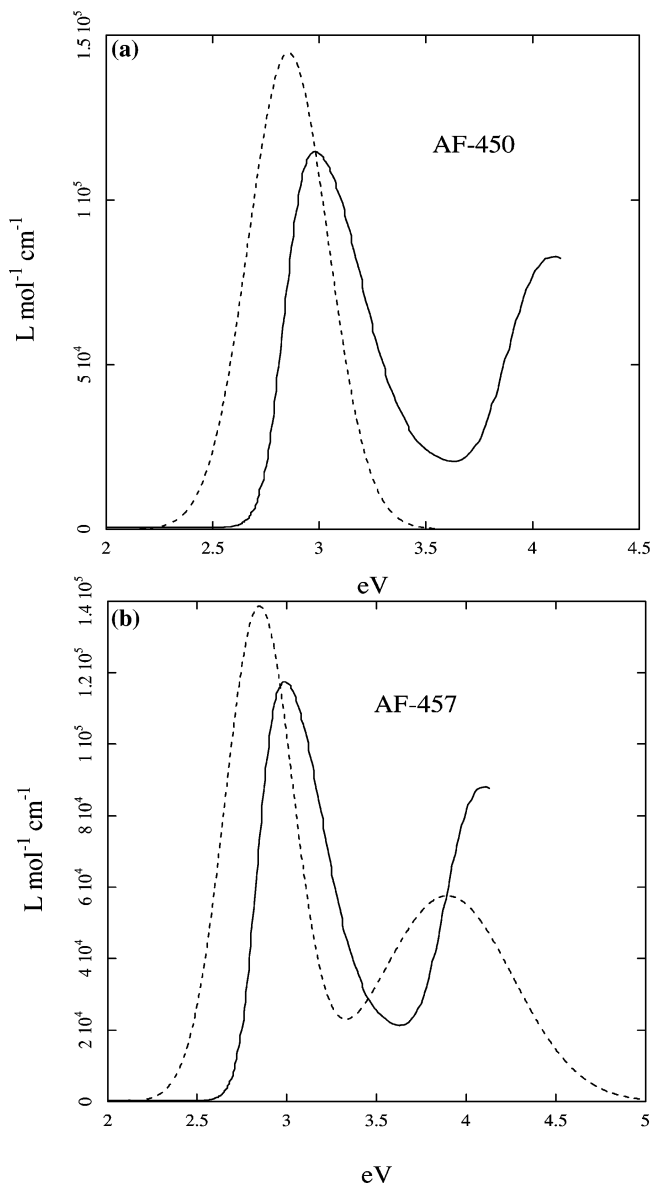
Figure 8. Experimental (in THF, solid) and computed (dash) OPA spectra of AF-450 (a, using fwhm = 0.45 eV for S_1) and AF-457 (b, using fwhm = 0.45 eV for S_1 and fwhm = 0.81 eV for S_2-S_n).

as compared to AF-380 in the same region of the OPA spectrum. In accordance with these predictions, the first maximum in the OPA spectrum of AF-459-2 is observed at 3.20 eV with ϵ_{max} of 2.46×10^5 L·mol^{-1}·cm^{-1} and $f = 3.33$. Thus, the second observed band (at 3.37 eV) is assigned to a vibrational progression. Another distinguishing feature that is verified in the observed spectrum is the weakness of the higher energy transitions. The second peak at 3.88 eV (ϵ_{max} of 4.14×10^4 L·mol^{-1}·cm^{-1}) is assigned to the third $^1E'$ state with the predicted excitation 3.84 eV and ϵ_{max} of 4.23×10^4 L·mol^{-1}·cm^{-1}. Because transitions higher than 4.01 eV were not computed, no assignment can be made for a third band. The tail in the simulated spectrum (Figure 10) reflects the lack of data beyond 4.01 eV.

Summary and Conclusions

In summary, the OPA spectra of the dipolar AF-270 and AF-240 are similar but differ markedly from those of the quadrupolar (i.e., AF-287, AF-295) and octupolar (i.e., AF-350, AF-380) congeners. All chromophores possess broad and intense

absorption bands. Except for AF-389, the order of excitation energies of their absorption bands is dipolar > quadrupolar > octupolar. This ordering is reversed for absorption intensities. These trends are common features in the two series with different conjugation lengths. Experiment and theory concur in this regard. The observed red-shifts in the multi-branched molecules are attributed to the stabilization of the LUMOs while the increased absorption intensities are attributed to electronic delocalization. However, a design for extending the conjugation length in AF-270, AF-295, and AF-350 by adding phenyl rings to AF240, AF-287, and AF380, respectively, does not produce significant changes in intensity for the first excited state due to the limited delocalization over the added phenyls. TDDFT calculations on AF-240 predict three $\pi-\pi^*$ transitions at energies <4 eV with an increase in the number of transitions for the quadrupolar and octupolar systems. Computations also indicate that two transitions underlie the lowest energy bands of the quadrupolar and octupolar systems whereas only one is predicted to underlie the corresponding band in the dipolar systems. No experimental estimates of the dipole moment (μ) of the ground state and excited state exist. The ground-state dipole moment varies as AF-240 (1.7 D) > AF-287 (1.4) > AF-380 (0.6 D); AF-270 (1.5 D) > AF-295 (1.3) > AF-350 (0.1 D). The one- and two-branched compounds are predicted to be highly polar, with the first transition accompanied by large $\Delta\mu$. Thus, the first excited states have ICT characteristics. The excited state ICT dipole moment varies as AF-240 (19.8 D) > AF-287 (9.1 D) > AF-380 (1.9 D); AF-270 (32.1 D) > AF-295 (14.5) > AF-350 (1.8 D). For the three-branched chromophores, the near C_{3h} symmetry greatly alters the polarities of the various electronic states and preludes the pure doubly degenerate S_1 electronic state assignments due to their near degeneracy with other states. Experimental spectral data are supportive of the conclusion of more than one transition in the lowest energy band envelope of the quadrupolar and octupolar chromophores. The TPA strength of DA chromophores can often be reasonably estimated by a two-state approximation, in which the TPA cross-section is proportional to the square of the $\Delta\mu$ between ground state and first excited state. Thus, based on the above values AF-270 is expected to exhibit strong TPA in to the first excited state. However, a quantitative treatment for TPA may involve additional states in the SOS expression and functionals with the correct $-1/r$ long-range behavior, which are currently under investigation.

Computations using TDDFT with the PBE0 functional for the series of fluorene-based D$-\pi-$A chromophores consistently underestimate the excitation energies, with a mean deviation of 0.16 eV for the first ICT bands in THF. Although PBE0 is generally well correlated with experiment, there are some large deviations. The largest deviation of 0.27 eV for AF-295 can be attributed to spectral broadening due to the convolution of a nearby electronic transition and, to a lesser degree, effects of solvent. Direct quantitative comparison with experimental oscillator strengths is not straightforward due to spectral broadening and band overlapping, which results in the lack of accurate absolute experimental values that can be assigned to individual electronic transitions. As noted, good agreement is observed in some cases. The computed and new experimental results help in resolving discordant experimental oscillator strengths in some cases, for example, AF-380, AF350, AF-270, and AF-295.

OPA of Fluorene-Based Chromophores

J. Phys. Chem. A, Vol. 110, No. 49, 2006 **13181**
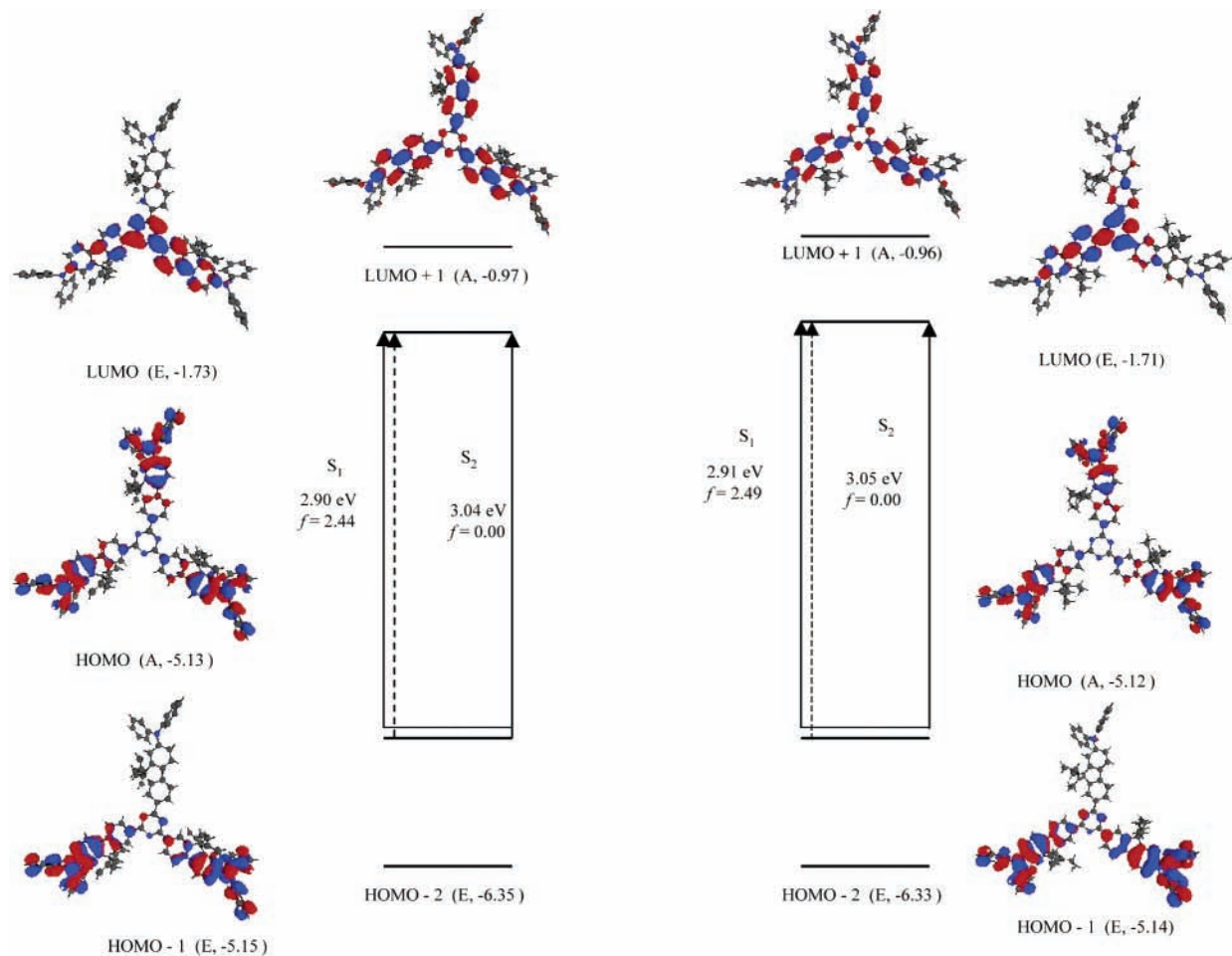
Figure 9. Molecular orbital diagrams for AF-450 and AF-457. Solid and broken arrows denote the major and minor one-electron excitations.
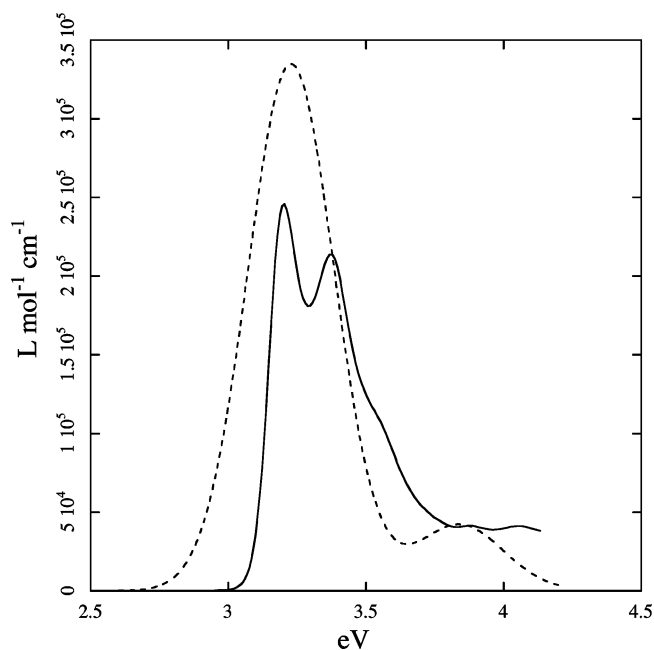
Figure 10. Experimental (in THF, solid) and computed (dash, using fwhm = 0.37 eV for S_1-S_n) OPA spectra of AF-459-2.

Finally, linear response TDDFT calculations predicted that the new AF-459-2 should absorb very strongly with first band maximum at 3.23 eV, and that absorption should be weak in the higher energy region. These predictions were confirmed by the synthesis and spectral characterization work. Second-order response TDDFT calculations are currently being carried out to obtain TPA cross-sections for these systems. The results will be reported in a future publication.

Supporting Information Available: Coordinates of all B3LYP/6-31G(d) optimized molecular structures; computed CAMB3LYP excitation energies and oscillator strengths. This material is available free of charge via the Internet at http://pubs.acs.org.

References and Notes

(1) Oudar, J. L.; Chemla, D. S. *J. Chem. Phys.* **1977**, *66*, 2664.

(2) Cheng, L.-T.; Wilson, T.; Stevenson, S. H.; Meredith, G. R.; Rikken, G.; Marder, S. R. *J. Phys. Chem.* **1991**, *95*, 10631.

(3) Cheng, L.-T.; Tam, W.; Marder, S. R.; Stiegman, A. E.; Rikken, G.; Spangler, C. W. *J. Phys. Chem.* **1991**, *95*, 10631.

(4) Rijkenberg, R. A.; Bebelaar, D.; Buma, W. J.; Hofstraat, J. W. *J. Phys. Chem. A* **2002**, *106*, 2446.

(5) Antonov, L.; Kamada, K.; Ohta, K.; Kamounah, F. *Phys. Chem. Chem. Phys.* **2003**, *5*, 1193.

(6) Spangler, C. W.; Starkey, J. R.; Meng, F.; Gong, A.; Drobizhev, M.; Rebane, A.; Moss, B. Optical methods for tumor treatment and detection: mechanisms and techniques in photodynamic therapy XIV. *Proc. SPIE—Int. Soc. Opt. Eng.* **2005**.

(7) Denk, W.; Strickler, J. H.; Webb, W. W. *Science* **1990**, *248*, 73.

Nguyen et al.

(8) Schafer-Hales, K. J.; Belfield, K. D.; Yao, S.; Federiken, P. K.; Hales, J. M.; Kolattukudy, P. E. *J. Biomed. Opt.* **2005**, *10*, 51402.

(9) Kirkpatrick, S. M.; Baur, J. W.; Clark, C. M.; Denny, L. R.; Tomlin, D. W.; Reinhardt, B. R.; Kannan, R.; Stone, M. O. *Appl. Phys. A: Mater. Sci. Process.* **1999**, *69*, 461.

(10) Reinhardt, B. A.; Brott, L. B.; Clarson, S. J.; Dillard, A. G.; Bhatt, J. C.; Kannan, R.; Yuan, L.; He, G. S.; Prasad, P. N. *Chem. Mater.* **1998**, *10*, 1863.

(11) Baur, J. W.; Alexander Jr., M. D.; Banach, M.; Denny, L.; Reinhardt, B. A.; Vaia, R. A.; Fleitz, P. A.; Kirkpatrick, S. M. *Chem. Mater.* **1999**, *11*, 2899.

(12) Belfield, K. D.; Hagan, D. J.; Van Stryland, E. W.; Schafer, K. J.; Negres, R. A. *Org. Lett.* **1999**, *1*, 1575.

(13) Belfield, K. D.; Schafer, K. J.; Liu, Y.; Liu, J.; Ren, X.; Van Stryland, E. W. *J. Phys. Org. Chem.* **2000**, *13*, 837.

(14) Kannan, R.; He, G. S.; Yuan, L.; Xu, F.; Prasad, P. N.; Dombroskie, A. G.; Reinhardt, B. A.; Baur, J. W.; Vaia, R. A.; Tan, L.-S. *Chem. Mater.* **2001**, *13*, 1896.

(15) Kannan, R.; He, G. S.; Lin, T.-C.; Prasad, P. N.; Vaia, R. A.; Tan, L.-S. *Chem. Mater.* **2004**, *16*, 185.

(16) He, G. S.; Lin, T.-C.; Prasad, P. N.; Kannan, R.; Vaia, R. A.; Tan, L.-S. *J. Phys. Chem. B* **2002**, *106*, 11081.

(17) He, G. S.; Lin, T.-C.; Dai, J.; Prasad, P. N.; Kannan, R.; Dombroskie, A. G.; Vaia, R. A.; Tan, L.-S. *J. Chem. Phys.* **2004**, *120*, 5275.

(18) He, G. S.; Swiatkiewicz, J.; Jiang, Y.; Prasad, P. N.; Reinhardt, B. A.; Tan, L.-S.; Kannan, R. *J. Phys. Chem. A* **2000**, *104*, 4810.

(19) Katan, C.; Terenziani, F.; Mongin, O.; Werts, M. H. V.; Porres, L.; Pons, T.; Mertz, J.; Tretiak, S.; Blanchard-Desce, M. *J. Phys. Chem. A* **2005**, *109*, 3024.

(20) Schafer, K. J.; Hales, J. M.; Balu, M.; Belfield, K. D.; Van Stryland, E. W.; Hagan, D. J. *J. Photochem. Photobiol. A* **2004**, *162*, 497.

(21) Swiatkiewicz, J.; Prasad, P. N.; Reinhardt, B. A. *Opt. Commun.* **1998**, *157*, 135.

(22) Rogers, J. E.; Slagle, J. E.; McLean, D. G.; Sutherland, R. L.; Sankaran, B.; Kannan, R.; Tan, L.-S.; Fleitz, P. A. *J. Phys. Chem. A* **2004**, *108*, 5514.

(23) Wang, C.-K.; Macak, P.; Agren, H. *J. Chem. Phys.* **2001**, *114*, 9813.

(24) Guo, J.-D.; Wang, C.-K.; Luo, Y.; Agren, H. *Phys. Chem. Chem. Phys.* **2003**, *5*, 3869.

(25) Day, P. N.; Nguyen, K. A.; Pachter, R. *J. Phys. Chem. B* **2005**, *109*, 1803.

(26) Rudberg, E.; Salek, P.; Helgaker, T.; Agren, H. *J. Chem. Phys.* **2005**, *123*, 184108.

(27) Burke, K.; Werschnik, J.; Gross, E. K. *J. Chem. Phys.* **2005**, *123*, 62206.

(28) Dreuw, A.; Head-Gordon, M. *Chem. Rev.* **2005**, *105*, 4009.

(29) Becke, A. D. *J. Chem. Phys.* **1993**, *98*, 5648.

(30) Becke, A. D. *Phys. Rev. A* **1988**, *38*, 3098.

(31) Lee, C.; Yang, W.; Parr, R. G. *Phys. Rev. B* **1988**, *37*, 785.

(32) Jamorski, C.; Foresman, J. B.; Thilgen, C.; Lüthi, H.-P. *J. Chem. Phys.* **2002**, *116*, 8761.

(33) Cave, R. J.; Burke, K.; Castner Jr., E. W. *J. Phys. Chem. A* **2002**, *106*, 9294.

(34) Cave, R. J.; Castner Jr., E. W. *J. Phys. Chem. A* **2002**, *106*, 12117.

(35) Tawada, Y.; Tsuneda, T.; Yanagisawa, S.; Yanai, T.; Hirao, K. *J. Chem. Phys.* **2004**, *120*, 8425.

(36) Yanai, T.; Tew, D. P.; Handy, N. C. *Chem. Phys. Lett.* **2004**, *393*, 51.

(37) Gritsenko, O.; Baerends, E. J. *J. Chem. Phys.* **2004**, *121*, 655.

(38) Heyd, J.; Scuseria, G. E. *J. Chem. Phys.* **2004**, *120*, 7274.

(39) Runge, E.; Gross, E. K. U. *Phys. Rev. Lett.* **1984**, *52*, 997.

(40) Bauernschmitt, R.; Ahlrichs, R. *Chem. Phys. Lett.* **1996**, *256*, 454.

(41) Casida, M.; Jamorski, C.; Casida, K. C.; Salahub, D. R. *J. Chem. Phys.* **1998**, *108*, 4439.

(42) Stratmann, R. E.; Scuseria, G. E.; Frisch, M. J. *J. Chem. Phys.* **1998**, *109*, 8218.

(43) Frisch, M. J.; Trucks, G. W.; Schlegel, H. B.; Scuseria, G. E.; Robb, M. A.; Cheeseman, J. R.; Montgomery, J. A., Jr.; Vreven, T.; Kudin, K. N.; Burant, J. C.; Millam, J. M.; Iyengar, S. S.; Tomasi, J.; Barone, V.; Mennucci, B.; Cossi, M.; Scalmani, G.; Rega, N.; Petersson, G. A.; Nakatsuji, H.; Hada, M.; Ehara, M.; Toyota, K.; Fukuda, R.; Hasegawa, J.; Ishida, M.; Nakajima, T.; Honda, Y.; Kitao, O.; Nakai, H.; Klene, M.; Li, X.; Knox, J. E.; Hratchian, H. P.; Cross, J. B.; Adamo, C.; Jaramillo, J.; Gomperts, R.; Stratmann, R. E.; Yazyev, O.; Austin, A. J.; Cammi, R.; Pomelli, C.; Ochterski, J. W.; Ayala, P. Y.; Morokuma, K.; Voth, G. A.; Salvador, P.; Dannenberg, J. J.; Zakrzewski, V. G.; Dapprich, S.; Daniels, A. D.; Strain, M. C.; Farkas, O.; Malick, D. K.; Rabuck, A. D.; Raghavachari, K.; Foresman, J. B.; Ortiz, J. V.; Cui, Q.; Baboul, A. G.; Clifford, S.; Cioslowski, J.; Stefanov, B. B.; Liu, G.; Liashenko, A.; Piskorz, P.; Komaromi, I.; Martin, R. L.; Fox, D. J.; Keith, T.; Al-Laham, M. A.; Peng, C. Y.; Nanayakkara, A.; Challacombe, M.; Gill, P. M. W.; Johnson, B.; Chen, W.; Wong, M. W.; Gonzalez, C.; Pople, J. A. *Gaussian 03*, revision A.11.4; Gaussian, Inc.: Pittsburgh, PA, 2003.

(44) Cossi, M.; Barone, V. *J. Chem. Phys.* **2001**, *115*, 4708.

(45) Cossi, M.; Scalmani, G.; Rega, N.; Barone, V. *J. Chem. Phys.* **2002**, *117*, 43.

(46) Schmidt, M., W.; Baldridge, K. K.; Boatz, J. A.; Elbert, S. T.; Gordon, M. S.; Jensen, J. H.; Koseki, S.; Matsunaga, N.; Nguyen, K. A.; Su, S.; Windus, T. L.; Dupuis, M.; Montgomery, J. A. *J. Comput. Chem.* **1993**, *14*, 1347.

(47) Bode, B. M.; Gordon, M. S. *J. Mol. Graphics Modell.* **1998**, *16*, 133.

(48) Press, W. H.; Flannery, B. P.; Teukolsky, S. A.; Vetterling, W. T. *Numerical Recipes, The Art of Scientific Computing*; Cambridge University: Cambridge, 1989.

(49) Dalton. a molecular electronic structure program, Release 2.0; http: www.kjemi.uio.no/software/dalton/dalton.html, 2005.

(50) Nifiatis, F.; Rogers, Private communication.

(51) Joshi, M. P.; Swiatkiewicz, J.; Xu, F.; Prasad, P. N.; Reinhardt, B. A.; Kannan, R. *Opt. Lett.* **1998**, *23*, 1742.

(52) Rumi, M.; Perry, J. W. Investigation of Air Force two-photon dyes. University of Arizona, 2002; Private communication.